MATHEMATICS OF COMPUTATION
Volume 76, Number 257, January 2007, Pages 361–384
S 0025-5718(06)01911-9
Article electronically published on October 4, 2006

DEFORMATION OF $\Gamma_0(5)$-CUSP FORMS

HELEN AVELIN

ABSTRACT. We develop an algorithm for numerical computation of the Eisenstein series on a Riemann surface of constant negative curvature. We focus in particular on the computation of the poles of the Eisenstein series. Using our numerical methods, we study the spectrum of the Laplace–Beltrami operator as the surface is being deformed. Numerical evidence of the destruction of $\Gamma_0(5)$-cusp forms is presented.

1. INTRODUCTION

Let Γ be a cofinite Fuchsian group acting on the Poincaré upper half-plane $\mathcal{H}$ equipped with the hyperbolic metric $ds^2 = y^{-2}(dx^2 + dy^2)$. When the surface $\Gamma\backslash\mathcal{H}$ is noncompact, i.e., has cusps, Selberg [34] showed that the Laplace–Beltrami operator

$$\Delta = y^2\left(\frac{\partial^2}{\partial x^2} + \frac{\partial^2}{\partial y^2}\right)$$

has both a discrete and a continuous spectrum. He showed in fact that the continuous spectrum is the interval $[1/4, \infty)$, which can be described naturally in terms of the Eisenstein series $E(z; s)$ with eigenvalue $\lambda = s(1-s)$. The discrete eigenfunctions are called Maass waveforms, and are known to be cusp forms whenever $\lambda \geq 1/4$.

An outstanding problem concerning the spectrum of Δ is whether for a general cofinite Fuchsian group Γ there exist infinitely many cusp forms on $\Gamma\backslash\mathcal{H}$. Vast progress on this question was made by Phillips and Sarnak [27, 28, 29], and in view of their work it is expected that for a generic Γ without special symmetries, there should be *no* cusp forms. In the present paper we will examine this question numerically by observing the spectrum as we start with a group Γ_0 which is known to have many cusp forms, and then deforming Γ_0 into groups Γ of "general" type in the Teichmüller space $T(\Gamma_0)$.

It is natural to choose Γ_0 to be a congruence subgroup of $PSL(2, \mathbb{Z})$. Our particular choice in this paper is $\Gamma_0 = \Gamma_0(5)$, a group which has recently been considered in a closely related context by Farmer and Lemurell [13]. The Teichmüller space $T(\Gamma_0)$ for this group is a two-dimensional manifold. Other choices of Γ_0 which would be interesting to study are (nonarithmetic) cycloidal subgroups of $PSL(2, \mathbb{Z})$ (cf., e.g., [21, 36]).

It turns out, as was expected, that the cusp forms are typically destroyed as the group is changed. Their destruction means that the Eisenstein series must sprout "compensatory" poles very close to $\mathrm{Re}\,(s) = 1/2$ (cf., e.g., [16], [29]). One of the

Received by the editor April 26, 2005 and, in revised form, January 30, 2006.
2000 *Mathematics Subject Classification.* Primary 11F72; Secondary 11F03, 11F06, 11Y35.

main goals of this work has been to track how these poles (known as resonances) *move* as the group is deformed. This appears to be the first time such tracking has ever been done.

Phillips and Sarnak conjecture that cusp forms are destroyed by *almost all* deformations in Teichmüller space. However, this does not exclude the possibility for cusp forms to be stable under deformation along certain paths in $T(\Gamma_0)$. These exceptional paths are the topic of numerical investigation in Farmer and Lemurell [13]. Their results suggest that for each cusp form there exists a curve in $T(\Gamma_0)$ along which the cusp form is not destroyed. Here, we are able to support their findings using our methods for tracking poles of the Eisenstein series. Using "Fermi's law" as proved by Phillips and Sarnak [29, 5.29], we are also able to explain rigorously an interesting property noted in the experiments of Farmer and Lemurell. Namely, the deformation curves are always tangent to a certain naturally described coordinate axis through the point Γ_0 in $T(\Gamma_0)$; cf. subsection 5.3 below.

Prior to explaining our algorithms in Section 4 and presenting our results in Section 5, we need to concern ourselves with some background material. In Section 2, we explain the technicalities of deforming the group, and Section 3 is devoted to deformation theory for cusp forms and Eisenstein series. Here we also present Lemma 3.1 which states a sufficient condition for cusp forms to be destroyed for *all* directions in Teichmüller space. However, our numerical results together with those of Farmer and Lemurell suggest that this condition should never be fulfilled, at least for the type of groups we consider.

2. The group $\Gamma_0(5)$ and some of its deformations

Let Γ_0 be a cofinite Fuchsian group acting on the Poincaré upper half-plane

$$\mathcal{H} = \{z = x + iy;\ y > 0\}$$

equipped with the hyperbolic metric $ds^2 = y^{-2}(dx^2 + dy^2)$. We will write the signature of Γ_0 as $(p, n; \nu_1, \ldots, \nu_n)$ if Γ_0 has n inequivalent elliptic or parabolic fixpoints of orders $\nu_1, \ldots, \nu_n$ and the topological space $\Gamma_0 \backslash \mathcal{H}$ has genus p. The Teichmüller space $T(\Gamma_0)$ is a real analytic manifold of topological dimension $\dim(T(\Gamma_0)) = 6p - 6 + 2n$; cf. [8, p. 275].

Our initial group will be

$$\Gamma_0 = \Gamma_0(5) = \left\{ \left(\begin{smallmatrix} a & b \\ c & d \end{smallmatrix}\right) \in PSL(2, \mathbb{Z})\,;\ c \equiv 0 \mod 5 \right\}$$

and its signature is $(0, 4; 2, 2, \infty, \infty)$; cf. [23, pp. 106–113]. This means that Γ_0 has two inequivalent elliptic fixpoints of order 2 and two inequivalent parabolic fixpoints (i.e., cusps). Also, it follows that $T(\Gamma_0(5))$ has dimension 2, and so there will be two real parameters to vary (at least locally near $\Gamma_0(5)$). We call these a and r and we will write $\Gamma_{a,r}$ (see precise definition below), or sometimes just Γ, for the deformations of Γ_0. We remark that (a, r) in fact provide real-analytic coordinates on $T(\Gamma_0(5))$ (with respect to its standard complex analytic structure), at least for $|a| < 0.05$ and $0.125 < r < 0.225$. A detailed proof of this is given in the Maple file [5], based on use of [25, §§2.2, 2.5, 3.1].

The specific deformation paradigm we shall use is a special case of [13]. Lemurell kindly shared their method with us at an early stage. Accordingly we will be working with the group

$$\widetilde{\Gamma}_0(5) = \langle \Gamma_0(5), W_0 \rangle, \tag{1}$$

where W_0 is the Fricke involution $z \mapsto -\frac{1}{5z}$. The point of this extension is two-fold: first, one has $[\widetilde{\Gamma}_0(5) : \Gamma_0(5)] = 2$ thanks to the relation

$$W_0^{-1}\Gamma_0(5)W_0 = \Gamma_0(5); \tag{2}$$

second, $\widetilde{\Gamma}_0(5)$ has only *one* cusp, the full signature being $(0, 4; 2, 2, 2, \infty)$.

A discussion of the generators of the groups $\Gamma_0(5)$, $\widetilde{\Gamma}_0(5)$, $\Gamma_{a,r}$ and $\widetilde{\Gamma}_{a,r}$ can be found in [13], where a more general case is considered, and in [4] where we have worked out the details for our special case. (Note that the parameters in [13] correspond to ours as $a = b_{FL}$ and $r = 1/a_{FL}$.) Here we simply state the generators of $\Gamma_{a,r}$ and $\widetilde{\Gamma}_{a,r}$ as follows.

$$S = \pm\begin{pmatrix}1 & 1\\ 0 & 1\end{pmatrix},\ W = \pm\begin{pmatrix}a & -r-a^2\\ 1 & -a\end{pmatrix},\ WSW = \pm\begin{pmatrix}1-\frac{a}{r} & \frac{a^2}{r}\\ -\frac{1}{r} & 1+\frac{a}{r}\end{pmatrix},$$

$$E = \pm\begin{pmatrix}\frac{a-2r-\sqrt{D}}{2} & \frac{(4r-1)a+(2a-1)\sqrt{D}}{2}\\ 1 & \frac{-a+2r+\sqrt{D}}{2}\end{pmatrix},$$

$$WEW = \pm\begin{pmatrix}\frac{a+2r+\sqrt{D}}{2} & \frac{(1-4r)a-(2a+1)\sqrt{D}}{2}\\ 1 & \frac{-a-2r-\sqrt{D}}{2}\end{pmatrix}, \text{where } D = 4r^2 + a^2$$

$$\widetilde{\Gamma}_{a,r} = \langle S, E, W\rangle \qquad (\text{relations} \quad W^2 = E^2 = (SEW)^2 = I),$$

$$\Gamma_{a,r} = \langle S, E, WEW, WSW\rangle \ (\text{relations} \ \ E^2 = (WEW)^2 = (SEW)^2 = I).$$

We obtain the groups $\Gamma_0(5)$ and $\widetilde{\Gamma}_0(5)$ when $(a, r) = (0, 1/5)$; i.e., $\Gamma_0(5) = \Gamma_{0,\frac{1}{5}}$ and $\widetilde{\Gamma}_0(5) = \widetilde{\Gamma}_{0,\frac{1}{5}}$.

In the Maple file [5] we give a careful proof that for $|a| < 0.05$ and $0.125 < r < 0.225$, the group $\Gamma_{a,r}$ is indeed Fuchsian with abstract presentation as in the last line of the box above. The main tool here is Poincaré's fundamental theorem; cf. [20]. More specifically, for any such a and r we give an explicit description of a convex geodesical polygon whose sides are identified in pairs by the isometries S, E, $R = WEW$, $T = WSW$, and we verify that all conditions in Poincaré's theorem are fulfilled. It follows that S, E, R, and T generate a Fuchsian group $\Gamma_{a,r}$ with presentation $\langle S, E, R, T | E^2 = R^2 = ETRS = I\rangle$; the last relation here is equivalent to $(SEW)^2 = I$. (The sides of the polygon are chosen to be the isometric circles of E, T^{-1}, T and R and the vertical lines $\mathrm{Re}\,(z) = \pm 1/2$. The main part of the proof in [5] is to show that for $|a| < 0.05$ and $0.125 < r < 0.225$ the locations and intersections of these circles are as expected. The angular cycle conditions needed in Poincaré's theorem are then easy to see—they follow in a rather formal way using the relations $E^2 = R^2 = ETRS$.) We also verify that $W \notin \Gamma_{a,r}$ and $W\Gamma_{a,r}W^{-1} = \Gamma_{a,r}$ hold. This implies that $\widetilde{\Gamma}_{a,r} := \langle \Gamma_{a,r}, W\rangle = \langle S, E, W\rangle$ contains $\Gamma_{a,r}$ as a normal subgroup of index 2; in particular $\widetilde{\Gamma}_{a,r}$ is Fuchsian too. Finally, it is then a simple exercise in abstract group theory to show that $\widetilde{\Gamma}_{a,r}$ has presentation as stated in the box.

Let $\mathcal{R}z$ denote the reflection $\mathcal{R}z = -\overline{z}$. A quick calculation with the generators shows that

$$\Gamma_{a,r} = \mathcal{R}\Gamma_{-a,r}\mathcal{R} \tag{3}$$

and, similarly, that

$$\widetilde{\Gamma}_{a,r} = \mathcal{R}\widetilde{\Gamma}_{-a,r}\mathcal{R}. \tag{4}$$

We define the character χ^- on $\widetilde{\Gamma}_{a,r}$ by

$$\chi^-(U) = 1 \quad \text{for } U \in \Gamma_{a,r}; \quad \chi^-(W) = -1. \tag{5}$$

Also let χ^+ denote the trivial character on $\widetilde{\Gamma}_{a,r}$.

There is a natural relation between functions on $\Gamma_{a,r}\backslash\mathcal{H}$ and functions on $\widetilde{\Gamma}_{a,r}\backslash\mathcal{H}$ with character. More precisely; any function f on $\Gamma_{a,r}\backslash\mathcal{H}$ can be *uniquely* written as $f^+ + f^-$, where $f^\pm(Lz) = \chi^\pm(L)f^\pm(z)$ for all $L \in \widetilde{\Gamma}_{a,r}$. In fact, $f^\pm(z) = \frac{1}{2}\left(f(z) \pm f(Wz)\right)$.

In the case of groups having $a = 0$ (i.e., $\Gamma_{0,r}$ and $\widetilde{\Gamma}_{0,r}$), it follows from equations (3) and (4) that functions can be decomposed further using the reflection $\mathcal{R}$: we call a function f on $L^2(\widetilde{\Gamma}_{0,r}\backslash\mathcal{H})$ *even* if $f(\mathcal{R}z) = f(z)$ and *odd* if $f(\mathcal{R}z) = -f(z)$. By the same method as above one verifies that every function f on $\widetilde{\Gamma}_{0,r}\backslash\mathcal{H}$ can be uniquely expressed as the sum of an even and an odd function on $\widetilde{\Gamma}_{0,r}\backslash\mathcal{H}$. The same is true on $\Gamma_{0,r}\backslash\mathcal{H}$.

Note that under the above splittings, L^2-functions decompose into L^2-functions and C^∞-functions into C^∞-functions, and eigenfunctions of the Laplace–Beltrami operator Δ decompose into eigenfunctions having the same eigenvalue (since Δ commutes with W and $\mathcal{R}$). In particular, if ϕ is a discrete eigenfunction on $\Gamma_{a,r}\backslash\mathcal{H}$ with eigenvalue λ (viz. $\phi \in L^2(\Gamma_{a,r}\backslash\mathcal{H}) \cap C^\infty(\mathcal{H})$ and $\Delta\phi + \lambda\phi = 0$), then $\phi(z) = \phi^+(z) + \phi^-(z)$ where ϕ^+ and ϕ^- are discrete eigenfunctions (possibly 0) on $\widetilde{\Gamma}_{a,r}\backslash\mathcal{H}$ with characters χ^+ and χ^-, respectively, and both having eigenvalue λ.

In the case $(a, r) = (0, \frac{1}{5})$, i.e., the congruence group $\Gamma_0(5) = \Gamma_{a,r}$, there are even more symmetries present. Recall that in view of [1] there will be two kinds of cusp forms on $\Gamma_0(5)$, oldforms and newforms. Oldforms arise in pairs $\phi(z)$ and $\phi(5z)$, where $\phi(z)$ is a cusp form on $PSL(2,\mathbb{Z})$ (cf. [22] or [37, Theorem 4.6], [39]).

The oldform $\phi(5z)$ has a very simple connection with the decomposition $\phi(z) = \phi^+(z) + \phi^-(z)$. In fact, by the invariance of $\phi(z)$ under $PSL(2,\mathbb{Z})$ we get

$$\phi^\pm(z) = \frac{\phi(z) \pm \phi(-\frac{1}{5z})}{2} = \frac{\phi(z) \pm \phi(5z)}{2}.$$

Also note that we have $\phi^\pm(W_0 z) = \pm\phi^\pm(z)$.

Regarding to the newforms on $\Gamma_0(5)$, these are expected to all occur with multiplicity one in the spectrum of Δ. We also remark that (irrespective of the multiplicity) there is no loss of generality in assuming that any basis elements already satisfy

$$\phi(W_0 z) = \pm\phi(z);$$

cf. [1, p. 147(Theorem 3(iii))].

3. Deformation theory and the Eisenstein series

In the previous section we have seen how our problem reduces to the case of eigenfunctions on $\widetilde{\Gamma}\backslash\mathcal{H}$ with character χ, where χ can be either χ^+ or χ^-.

While cusp forms correspond (for $\lambda \geq 1/4$) to the discrete spectrum of the Laplace–Beltrami operator Δ on $\widetilde{\Gamma}\backslash\mathcal{H}$, the continuous spectrum arises from the

Eisenstein series; cf. [15, 18]. In our situation one defines

$$E(z;s;\chi) = \sum_{U\in\langle S\rangle\backslash\widetilde{\Gamma}} \chi(U)(\operatorname{Im} Uz)^s \tag{6}$$

for $\operatorname{Re}(s) > 1$. Note here that $\chi(S) = 1$, since $S \in \Gamma_{a,r}$ and $\chi^{\pm}[\Gamma_{a,r}] = 1$ (cf. (5) and the box on p. 363). It is customary to expand $E(z;s;\chi)$ in a Fourier series as

$$E(z;s;\chi) = y^s + \varphi(s)y^{1-s} + \sum_{\substack{m=-\infty\\ m\neq 0}}^{\infty} \varphi_m(s)y^{1/2}K_{s-1/2}(2\pi|m|y)e^{2\pi imx}. \tag{7}$$

Let $\phi(z)$ be a cusp form on $L^2(\widetilde{\Gamma}_0,\chi)$ of multiplicity one with eigenvalue $\lambda_0 = s_0(1-s_0) = 1/4 + R_0^2$. We will use the fact that *if* $\phi(z)$ is destroyed when $\widetilde{\Gamma}_0$ is deformed into $\widetilde{\Gamma}$, it must necessarily create a pole ξ of the Eisenstein series $E(z;s;\chi)$ close to s_0 and lying within $\{\operatorname{Re}(s) < 1/2\}$ (cf. [16, pp. 6, 95], [15, pp. 231, 143–148] and [29]).

It is known that the pole's dependence on the Teichmüller parameters of $\widetilde{\Gamma}$ is real-analytic (cf. Phillips and Sarnak [29]). In fact a stronger statement is true, namely the real-analyticity of the *singular set*, $\sigma(\widetilde{\Gamma})$, in Teichmüller space. We recall the result for the case of multiplicity one cusp forms having $\lambda > 1/4$. Assume $\operatorname{Re}(u) \neq 0$; then u belongs to $\sigma(\widetilde{\Gamma})$ if and only if $\operatorname{Im}(u) = 0$ and $\lambda = 1/4 + u^2$ is an eigenvalue of a cusp form on $\widetilde{\Gamma}_0\backslash\mathcal{H}$, *or* $\operatorname{Im}(u) > 0$ and $s = 1/2 + iu$ is a pole of $\varphi(s)$. Now by [29], if $\lambda = 1/4 + u_0^2$ is the eigenvalue of a cusp form of multiplicity one on $\widetilde{\Gamma}_0\backslash\mathcal{H}$, then there is a unique real-analytic function $u(a,r)$ in some neighborhood of $(a,r) = (0,1/5)$ such that $u(a,r) \in \sigma(\tilde{\Gamma}_{a,r})$ and $u(0,1/5) = u_0$. The motivation for the definition of $\sigma(\Gamma)$ is the Selberg trace formula (cf. also [15, p. 229–231]).

In particular the pole ξ of the Eisenstein series $E(z;s;\chi)$ varies real-analytically with our Teichmüller parameters a and r, and if the cusp form is *not* destroyed, its eigenvalue varies real-analytically with a and r.

We shall seek to find the pole ξ, and track it under various deformations $\widetilde{\Gamma}_0 \longrightarrow \widetilde{\Gamma}$. If we *do* find a reasonable path of poles moving away from s_0, this is clearly strong evidence that the cusp form $\phi(z)$ *is* indeed destroyed as $\widetilde{\Gamma}_0 \longrightarrow \widetilde{\Gamma}$. Repeating the procedure for $\chi = \chi^+$ and $\chi = \chi^-$, we are able to draw the same conclusion also as $\Gamma_0 \longrightarrow \Gamma$ thanks to the decomposition $\phi(z) = \phi^+(z) + \phi^-(z)$ introduced in Section 2 for functions on $\Gamma\backslash\mathcal{H}$.

The poles of $E(z;s;\chi)$ in $\{\operatorname{Re}(s) < 1/2\}$ coincide with those of the function $\varphi(s)$ (cf. [15, p. 255(4.4)] and (7)). Furthermore we have the standard relations

$$E(z;s;\chi) = \varphi(s)E(z;1-s;\chi), \quad \varphi(s)\varphi(1-s) = 1$$

applicable over any one-cusp group (see [15, pp. 77, 130]), which implies that ξ is a pole of $\varphi(s)$ if and only if $1-\xi$ is a zero. Using the fact that $\varphi(s)$ is real for real s (cf. [15, p. 66 (Remark 8.7)]) we get from the reflection principle that $1-\overline{\xi}$ is also a zero of $\varphi(s)$. We will track the zeros

$$\rho \equiv \frac{1}{2} + \eta + i\gamma$$

of $\varphi(s)$ in $\{\operatorname{Re}(s) > 1/2\}$ rather than poles of $E(z;s;\chi)$ (equivalently, poles of $\varphi(s)$) in $\{\operatorname{Re}(s) < 1/2\}$. Computationally, zeros are easier to deal with than poles, so

this seems like a natural choice. The poles are then given by $\xi = 1/2 - \eta + i\gamma$, and the corresponding point in the singular set $\sigma(\widetilde{\Gamma})$ is $u = \gamma + i\eta$.

Since u is a real-analytic function of a, r, we may expand η and γ in Taylor series as functions of a and r. We start out at a cusp form $\phi(z)$ with eigenvalue corresponding to $s_0 = 1/2 + iR_0$ (which means that $\eta = 0$ and $\gamma = R_0$) at $(a, r) = (0, 1/5)$. The symmetry relation $\widetilde{\Gamma}_{a,r} = \mathcal{R}\widetilde{\Gamma}_{-a,r}\mathcal{R}$ mentioned in Section 2 implies that a should only appear with even powers. Also note that in this notation we have $\mathrm{Im}\,(u) = \eta$, and u-values with $\mathrm{Re}\,(u) \neq 0$, $\mathrm{Im}\,(u) < 0$ do not belong to $\sigma(\widetilde{\Gamma})$; thus we will always have $\eta \geq 0$. So the Taylor expansions *must* take the form (near $a = 0$, $r = 1/5$, and $s_0 = 1/2 + iR_0$):

$$\begin{aligned}\eta =& A_1 a^2 + A_2(r - \tfrac{1}{5})^2 + A_3 a^2(r - \tfrac{1}{5}) + A_4(r - \tfrac{1}{5})^3 \\ &+ A_5 a^4 + A_6 a^2(r - \tfrac{1}{5})^2 + A_7(r - \tfrac{1}{5})^4 + A_8 a^4(r - \tfrac{1}{5}) \\ &+ A_9 a^2(r - \tfrac{1}{5})^3 + A_{10}(r - \tfrac{1}{5})^5 + A_{11} a^6 + \cdots, \end{aligned} \tag{8}$$

$$\begin{aligned}\gamma =& R_0 + B_0(r - \tfrac{1}{5}) + B_1 a^2 + B_2(r - \tfrac{1}{5})^2 \\ &+ B_3 a^2(r - \tfrac{1}{5}) + B_4(r - \tfrac{1}{5})^3 + B_5 a^4 + \cdots \end{aligned} \tag{9}$$

with $A_1 \geq 0$, $A_2 \geq 0$. Any "path numerics" can thus be fitted to an *a priori* pattern locally. The more stable the values in this, the greater the likelihood that $\phi(z)$ is destroyed *and* that the pole of $E(z; s; \chi)$ in $1 - \overline{\rho}$ is a remnant thereof.[1]

It is expected from [27] that cusp forms are destroyed for almost all deformations of the group and one of our main goals was to find numerical evidence of this phenomenon. However, the Taylor expansions above may also be used to tell whether $\phi(z)$ is destroyed for *all* directions in Teichmüller space. The following lemma states a first sufficient condition for this.

Lemma 3.1. *Let $\eta(a, r)$ be as in* (8) *and let*

$$\begin{aligned}P_4(a, r) = A_1 a^2 + A_2(r - \tfrac{1}{5})^2 + A_3 a^2(r - \tfrac{1}{5}) + A_4(r - \tfrac{1}{5})^3 \\ + A_5 a^4 + A_6 a^2(r - \tfrac{1}{5})^2 + A_7(r - \tfrac{1}{5})^4\end{aligned}$$

be the fourth-order Taylor approximation of $\eta(a, r)$. Suppose $A_1 = 0$ and $A_2 > 0$. Then we necessarily have

$$4A_2A_5 - A_3^2 \geq 0.$$

Furthermore, if $4A_2A_5 - A_3^2 > 0$, then both $P_4(a, r) > 0$ and $\eta(a, r) > 0$ hold in some punctured neighborhood of $(a, r) = (0, 1/5)$.

(The condition $A_1 = 0$ is not unrealistic; cf. subsection 5.3.)

Farmer and Lemurell [13] use a different approach to explore the possibility of complete destruction of cusp forms. In fact, they are able to track what seems to be stable cusp forms as the group is deformed. They conjecture that for every cusp form on a noncompact Riemann surface with nontrivial Teichmüller space there is a continuous family of Teichmüller deformations on which the cusp form lives. In view of Lemma 3.1 this suggests that we should actually always have $4A_2A_5 - A_3^2 = 0$.

[1] Also that there are *no* further poles of $E(z; s; \chi)$ near $1/2 + iR_0$; cf. (13) on page 373 and [29, (1.1)].

Proof of Lemma 3.1. We will use a change of variable and write $r - 1/5 = ua^2$. With our new variables P_4 becomes

$$P_4(a, \tfrac{1}{5} + ua^2) = (A_2u^2 + A_3u + A_5)a^4 + (A_4u^3 + A_6u^2)a^6 + A_7u^4a^8.$$

Fix u and let $a \to 0$. Note that because P_4 is the fourth-order Taylor approximation of η we have

$$|\eta(a, r) - P_4(a, r)| \leq C(a^2 + (r - \tfrac{1}{5})^2)^{5/2} = C(a^2 + (ua^2)^2)^{5/2} \leq C'|a|^5.$$

Hence $\eta(a, \frac{1}{5} + ua^2) = (A_2u^2 + A_3u + A_5)a^4 + O(a^5)$, and using this in conjunction with $\eta(a, \frac{1}{5} + ua^2) \geq 0$ as $a \to 0$ (dividing through by a^4), we obtain

$$A_2u^2 + A_3u + A_5 \geq 0.$$

Note that this holds for *all* real u; hence by completing the square (using $A_2 > 0$) we find

$$4A_2A_5 - A_3^2 \geq 0.$$

We now assume $4A_2A_5 - A_3^2 > 0$, and we will prove that $P_4(a, r) > 0$ and $\eta(a, r) > 0$ in some punctured neighborhood of $(a, r) = (0, 1/5)$.

We begin with the case $b_1a^2 < |r - 1/5| < b_2$, where b_1, b_2 are some suitable, positive constants depending on $A_2, A_3, \ldots, A_7$. In this region we do not need the fact that $4A_2A_5 - A_3^2 > 0$ for here we can achieve the following estimates:

$$|A_3a^2(r - \tfrac{1}{5})| < \frac{1}{10}A_2(r - \tfrac{1}{5})^2, \qquad |A_4(r - \tfrac{1}{5})^3| < \frac{1}{10}A_2(r - \tfrac{1}{5})^2,$$
$$|A_5a^4| < \frac{1}{10}A_2(r - \tfrac{1}{5})^2, \qquad |A_6a^2(r - \tfrac{1}{5})^2| < \frac{1}{10}A_2(r - \tfrac{1}{5})^2,$$
$$|A_7(r - \tfrac{1}{5})^4| < \frac{1}{10}A_2(r - \tfrac{1}{5})^2.$$

So we get

$$P_4(a, r) > \frac{1}{2}A_2(r - \tfrac{1}{5})^2 > 0,$$

(using $|r - 1/5| > b_1a^2 \geq 0$) and, for $|r - 1/5|$ small enough,

$$\eta(a, r) > \frac{1}{2}A_2(r - \tfrac{1}{5})^2 - C|r - \tfrac{1}{5}|^{5/2} > 0.$$

It remains to treat the region $|u| \leq b_1$. Here we will use the strict inequality $4A_2A_5 - A_3^2 > 0$. We find

$$\begin{aligned} P_4(a, \tfrac{1}{5} + ua^2) &= (A_2u^2 + A_3u + A_5)a^4 + (A_4u^3 + A_6u^2)a^6 + A_7u^4a^8 \\ &\geq \left(A_2\left(u + \frac{A_3}{2A_2}\right)^2 + \frac{4A_2A_5 - A_3^2}{4A_2}\right)a^4 - \left|\left(A_4u^3 + A_6u^2\right)a^6\right| - \left|A_7u^4a^8\right| \\ &\geq \left(\frac{4A_2A_5 - A_3^2}{4A_2}\right)a^4 - \left(|A_4|b_1^3 + |A_6|b_1^2\right)a^6 - |A_7|b_1^4a^8. \end{aligned}$$

This is clearly positive for a small enough when $4A_2A_5 - A_3^2 > 0$. Similarly

$$\eta(a, \tfrac{1}{5} + ua^2) > \left(\frac{4A_2A_5 - A_3^2}{4A_2}\right)a^4 - C|a|^5 > 0$$

for small a. $\square$

Note that if $4A_2A_5 - A_3^2 = 0$, the proof of Lemma 3.1 gives $\eta(a,r) = O(a^6)$ along any curve of the form $r = 1/5 - \frac{A_3}{2A_2}a^2 + O(a^4)$. This confirms the remark in Farmer and Lemurell [13, section 4.6] about sixth-order contact: In our coordinates the predicted curve in [13] is $r = 1/5 - 2.66916a^2 + O(a^4)$ for $R_0 = 5.4362$. Using $A_2 = 244.881668$ and $A_3 = 1307.25768$, which are found with the methods for high precision computations of Maass forms developed in [9] (cf. subsection 5.5), we get $\frac{A_3}{2A_2} = 2.66916197$. The agreement with [13] is certainly striking.

We end this section with a few remarks on the Eisenstein series on $\Gamma_{a,r}$ and their relation to the Eisenstein series on $\widetilde{\Gamma}_{a,r}$. The group $\Gamma_{a,r}$ has two cusps, a and $i\infty$, and there is one Eisenstein series corresponding to each one of these cusps. They will be denoted $E_a(z;s;\Gamma)$ and $E_{i\infty}(z;s;\Gamma)$. Using that $W(i\infty) = a$ and $W\Gamma W^{-1} = \Gamma$, we find that

$$E_a(z;s;\Gamma) = E_{i\infty}(Wz;s;\Gamma). \tag{10}$$

A simple analysis using Section 2 and [15, Chap. 8 proposition 3.7] (i.e., the Fourier expansion) then shows that

$$E(z;s;\chi^{\pm}) = E_{i\infty}(z;s;\Gamma) \pm E_a(z;s;\Gamma). \tag{11}$$

When $a = 0$, one readily checks that all these Eisenstein series are "even" in the sense of Section 2. (It suffices to evaluate $E(z;s;\chi^{\pm})$ in two ways and then average: first with U, then with $\mathcal{R}U\mathcal{R}$ in (6); cf. also (4).)

Another important fact that is readily checked, this time by combining (10) and (11) with [15, pp. 280–281], is that the determinant of the 2×2 scattering matrix $\Phi(s)$ for $\Gamma_{a,r}$ is simply $\varphi^+(s)\varphi^-(s)$;

$$\det(\Phi(s)) = \varphi^+(s)\varphi^-(s),$$

where $\varphi^{\pm}(s)$ corresponds to $E(z;s;\chi^{\pm})$ in the obvious way (cf. (7)).

4. The algorithm

4.1. **Computing cusp forms and Eisenstein series on groups with one cusp.** In this section, we present the essential ideas for computations of cusp forms and Eisenstein series. Our computations of the Eisenstein series were made by amplifying on the algorithm developed by Hejhal [17] for computation of cusp forms on a Fuchsian group with one cusp. Though the underlying methodology remains one of linear algebra *combined with* finite Fourier series, three important revisions are called for. Specifically:

1. The algebra needs to be updated to accommodate the "$n = 0$" term $y^s + \varphi(s)y^{1-s}$.
2. The K-Bessel function algorithm needs to be extended from $K_{iR}(X)$ to $K_{s-\frac{1}{2}}(X)$ with $s \in \mathbb{C}$.
3. All arithmetic needs to be converted from real to complex.

Our program computes the functions $E(z;s;\chi^+)$ and $E(z;s;\chi^-)$ as Fourier series; we thus get the key values $\varphi^+(s)$ and $\varphi^-(s)$ automatically. Our algorithm will be explained below; the code itself can be found in [3].

We will use the Fourier expansion (cf. (7)). It is known that the K-Bessel function $K_{s-\frac{1}{2}}(X)$ decays exponentially fast with X (cf. [12, p. 86(7)]) and from

[24, Lemma 2.7] we have the bound (cf. (7))

$$\varphi_m(s) = O\left(|m|^{\frac{1}{2}+\left|\mathrm{Re}\,(s)-\frac{1}{2}\right|+\varepsilon}\right)$$

(where the implied constant depends on s and Γ). These two facts together imply that we can find an $M(y)$ such that

$$E(z;s;\chi) = A(y) + \sum_{m=-M(y)}^{M(y)} c_m(y)e^{2\pi imx} + [[\varepsilon]],$$

where $[[\varepsilon]]$ has an absolute value less than ε (for work on the computer, we think of ε as being 10^{-16}) and

$$\begin{aligned} &A(y) = y^s, && c_m(y) = c_m k_m(y), \\ &c_0 = \varphi(s), && k_0(y) = y^{1-s}, \\ &c_m = \varphi_m(s), && k_m(y) = y^{1/2}K_{s-1/2}(2\pi|m|y), \quad \text{for } m \neq 0. \end{aligned}$$

Now let $Y_{\min} = \min\{\mathrm{Im}\,(z)\,;\ z \in \mathcal{F}\}$ where $\mathcal{F}$ is the fundamental region of Γ, and set $M_0 = M(Y_{\min})$. Fix any $Y < Y_{\min}$, and then keep $Q \geq M(Y) + 1$. Consider $2Q$ equally spaced points

$$z_j = x_j + iY \quad \text{where } x_j = \frac{j - 1/2}{2Q},\ j = 1-Q, \ldots, Q.$$

Neglecting any terms like $[[\varepsilon]]$, we may now use a finite Fourier transform to solve for the coefficients $\varphi_m(s)$ of $E(z;s;\chi)$ (for $-M_0 \leq m \leq M_0, m \neq 0$):

$$\frac{1}{2Q}\sum_{j=1-Q}^{Q} E(z_j;s;\chi)e^{-2\pi imx_j} = \begin{cases} A(Y) + c_0(Y), & m = 0, \\ c_m(Y), & m \neq 0. \end{cases}$$

The next step is to use the automorphy of $E(z;s;\chi)$ under the group $\widetilde{\Gamma}$. Denote by z_j^* the image of z_j in $\mathcal{F}$ and write $z_j^* = T_j(z_j)$. For $m \neq 0$ (and entirely similar for $m = 0$) this leads to

$$\begin{aligned} c_m(Y) &= \frac{1}{2Q}\sum_{j=1-Q}^{Q} \chi(T_j)E(z_j^*;s;\chi)e^{-2\pi imx_j} \\ &= \frac{1}{2Q}\sum_{j=1-Q}^{Q} \chi(T_j)\left(A(y_j^*) + \sum_{n=-M_0}^{M_0} c_n(y_j^*)e^{2\pi inx_j^*}\right)e^{-2\pi imx_j} \\ &= \frac{1}{2Q}\sum_{j=1-Q}^{Q} \chi(T_j)A(y_j^*)e^{-2\pi imx_j} \\ &\qquad + \frac{1}{2Q}\sum_{n=-M_0}^{M_0} c_n \sum_{j=1-Q}^{Q} \chi(T_j)k_n(y_j^*)e^{2\pi inx_j^*}e^{-2\pi imx_j}. \end{aligned}$$

The final system of equations is, for $m = -M_0, \ldots, M_0$,

$$\sum_{n=-M_0}^{M_0} c_n \widetilde{V}_{mn} = -\widetilde{A}_m,$$

where

$$\widetilde{A}_m = \frac{1}{2Q} \sum_{j=1-Q}^{Q} \chi(T_j) A(y_j^*) e^{-2\pi i m x_j} - \delta_{m0} A(Y),$$

$$\widetilde{V}_{mn} = \frac{1}{2Q} \sum_{j=1-Q}^{Q} \chi(T_j) k_n(y_j^*) e^{2\pi i n x_j^*} e^{-2\pi i m x_j} - \delta_{mn} k_m(Y).$$

The system depends on Y and M_0, but, of course, the result should be independent of these values as long as they are chosen within the permitted bounds.

The main difficulty here is that the K-Bessel function $K_{s-1/2}(X)$ has *complex* order because we deal with arbitrary $s \in \mathbb{C}$ (near $\mathrm{Re}\,(s) = 1/2$). For cusp forms, the corresponding K-Bessel functions have purely imaginary order, and Hejhal has developed algorithms to compute them; cf. [16, p. 125].

Based on the same ideas, we have built an algorithm for $K_{s-1/2}(X)$ with $s \in \mathbb{C}$ near $1/2 + iR$. This is explained in subsection 4.3.

We have also implemented a program for computing cusp forms with Hejhal's algorithm for groups with one cusp. In one aspect it is easier to compute $E(z; s; \chi)$ than cusp forms: because $E(z; s; \chi)$ exists for every s, we never have to *search* for eigenvalues.

4.2. **Finding zeros.** Our aim is to find the zeros of $\varphi(s)$ inside a rectangle A given by $\sigma_1 < \mathrm{Re}\,(s) < \sigma_2$, $0 < R_1 < \mathrm{Im}\,(s) < R_2$, with $\sigma_1 \geq 1/2$. We know that there are no poles of $\varphi(s)$ in $\mathrm{Re}\,(s) \geq 1/2$, $\mathrm{Im}(s) \neq 0$, and we will assume that there is exactly one zero, s_0, inside A (we can check the number of zeros with the argument principle and split A if necessary), and that $\varphi(s) \neq 0$ along ∂A. From the Cauchy residue theorem we have

$$2\pi i s_0 = \int_{\partial A} s \, \frac{\varphi'(s)}{\varphi(s)} \, ds,$$

where the integral is counterclockwise around A. Integrating this by parts we find

$$\int_{\partial A} s \, \frac{\varphi'(s)}{\varphi(s)} \, ds = 2\pi i(\sigma_1 + iR_1) - \int_{\partial A} \log \varphi(s) \, ds,$$

where we have used the branch cut along the ray from s_0 through $\sigma_1 + iR_1$, and we start integrating at $\sigma_1 + iR_1$. Our final result becomes

$$s_0 = (\sigma_1 + iR_1) - \frac{1}{2\pi i} \int_{\partial A} \log \varphi(s) \, ds,$$

and this integral is what we compute to find s_0. This is done using Gaussian quadrature with Legendre polynomials of degree 16 (cf., e.g., [31]). In calculating $\log \varphi(s)$, we need $\arg \varphi(s)$. So without any additional effort, we can use the argument principle to check that the number of zeros inside the rectangle does not exceed one. Ultimately we may use a variation of Newton's method with our zero as input to get higher accuracy. Unfortunately, with $\varphi(s)$, we found that Newton's method does not converge unless the input is already very close to the zero. (Exactly how close varies a lot, but typically we need about three correct decimals to get convergence.) This is why the first step is necessary.

4.3. **The K-Bessel function.** The K-Bessel function is defined by (cf. [42, p. 181])

$$K_\nu(X) = \frac{1}{2}\int_{-\infty}^{\infty} e^{-X\cosh t} e^{\nu t} dt.$$

We will put $\nu = A + iR$ $(A, R \in \mathbb{R})$ and rewrite this as

$$K_\nu(X) = \frac{1}{2}\int_{-\infty}^{\infty} e^{At} e^{\psi(t)} dt,$$

with $\psi(t) = -X\cosh t + iRt$. The idea is to change the path of integration in line with the method of stationary phase and then integrate numerically. This means that we will integrate over a curve along which $\operatorname{Im}\psi(t)$ is constant and $\operatorname{Re}\psi(t)$ has a maximum. The choice of this curve depends on the magnitude of $T = R/X$. We get three cases: $T < 1$, $T \approx 1$, and $T > 1$. We will consider A to be a small perturbation and we will always keep $|A| \leq 2$. Changing the path like this ensures us that we will get the bulk of the value of the integral even if we integrate over just a small portion of the path. We are also able to approximate the error term to know how far we need to integrate along the path to get the desired accuracy.

To give a taste of the method, we will show how to obtain the path of integration for the case $T > 1$. (For a reference on the method of stationary phase in relation to Bessel functions, see [42, p. 235].)

To find a point where $\operatorname{Re}\psi(t)$ has a maximum, we solve $\psi'(t) = 0$. Two solutions are found:

$$\begin{aligned} t_1 &= \ln\left(T + \sqrt{T^2 - 1}\right) + i\frac{\pi}{2}, \\ t_2 &= -\ln\left(T + \sqrt{T^2 - 1}\right) + i\frac{\pi}{2}. \end{aligned}$$

We will choose to consider the solution t_1. We want to find a curve through t_1 along which $\operatorname{Im}\psi(t)$ is constant. To do this, we let $t = u + iv$ and write

$$\begin{aligned} \psi(u + iv) &= U(u + iv) + iV(u + iv) \\ &= -X\cosh u\cos v - Rv + i(Ru - X\sinh u\sin v). \end{aligned}$$

The condition $\operatorname{Im}\psi(t) =$ constant along the curve is then

$$V(t) = V(t_1),$$

which becomes

$$\begin{aligned} Ru - X\sinh u\sin v &= R\ln\left(T + \sqrt{T^2 - 1}\right) - X\sinh\left(\ln\left(T + \sqrt{T^2 - 1}\right)\right)\sin\frac{\pi}{2} \\ &= R\ln\left(T + \sqrt{T^2 - 1}\right) - X\sqrt{T^2 - 1}. \end{aligned}$$

We rearrange this to find that the path is given by (recall that $T = R/X$)

$$\sin v = \frac{Tu - T\ln\left(T + \sqrt{T^2 - 1}\right) + \sqrt{T^2 - 1}}{\sinh u}. \tag{12}$$

We expand $\psi(t)$ in a Taylor series around t_1 to see what it looks like along this curve:

$$\begin{aligned}\psi(t) &= \psi(t_1) + \frac{\psi''(t_1)}{2}(t-t_1)^2 + O\left((t-t_1)^3\right)\\ &= -R\frac{\pi}{2} + i\left[R\ln\left(T+\sqrt{T^2-1}\right) - X\sqrt{T^2-1}\right]\\ &\quad - \frac{iX}{2}\sqrt{T^2-1}\,(t-t_1)^2 + O\left((t-t_1)^3\right).\end{aligned}$$

We find that the amplitude of $K_\nu(X)$ behaves like $e^{-R\frac{\pi}{2}}$ for large R. So it decays exponentially as R grows. This could cause problems in our program. To compensate we will instead compute $e^{R\frac{\pi}{2}}K_\nu(X)$, which will behave like $O(1)$ when R is big.

The presence of the factor $\sqrt{T^2-1}$ shows why it is necessary to divide into the cases $T<1$ and $T>1$. When $|R-x| < 5^{2/3}R^{1/3}$, we use the third case $T \approx 1$.

We now state precisely what paths were used in the three cases. Note that (12) is only valid as long as the right-hand side is less than 1. For $u < u_0$, where

$$u_0 = \ln\left(T+\sqrt{T^2-1}\right) - \frac{\sqrt{T^2-1}}{T},$$

this is no longer fulfilled ($u_0 < u_1$ automatically holds). So we need a different path for $0 < u < u_0$ and here we use just a horizontal line; $v = \pi$ is the one that makes the curve continuous at u_0. The paths used in our program are given by the relations

- $T > 1$:
  $$v = \pi, \qquad 0 < u < u_0,$$
  $$\sin v = \frac{Tu - T\ln\left(T+\sqrt{T^2-1}\right) + \sqrt{T^2-1}}{\sinh u}, \qquad u > u_0;$$
- $T < 1$: $$\sin v = \frac{Tu}{\sinh u}, \qquad u > 0;$$
- $T \approx 1$: $$\sin v = \frac{u}{\sinh u}, \qquad u > 0.$$

The same paths are used in [16].

In the end, the integral is computed using Gaussian quadrature with Legendre polynomials of degree 16 (cf., e.g., [31]).

Our program for $e^{R\frac{\pi}{2}}K_{A+iR}(X)$ is expected to give between 9- and 15-place accuracy depending on the size of R. It is designed to work in the ranges $0 \le R \le 100\,000$, $X \ge 1/5$ and $|A| \le 2$, but if other parameters are needed, one may adapt the error analysis. In our present work, R is always kept relatively small, and we expect the program to give 15 accurate places for $R < 20$ and 14 places for $R < 100$. The tests we ran are described in subsection 4.5.

4.4. **The pull-back algorithm.** The algorithms for cusp forms and $E(z;s;\chi)$ both require the image, or the pull-back, $z^* \in \mathcal{F}$, in the fundamental region, of a point $z \in \mathcal{H}$ (cf. p. 369).

The fundamental region $\mathcal{F}$ of $\widetilde{\Gamma}$ has finitely many sides; cf. [5]. Assume that the sides of $\mathcal{F}$ are the isometric circles of $T_1, T_2, \ldots, T_n$. The following algorithm will provide the pull-back in the fundamental region of a point z. (This algorithm

seems to be well known among experts in the field, but we are not aware of any description in the literature. In a related vein see [38].)

1. Let $z \in \mathcal{H}$ with $|\mathrm{Re}\,(z)| \leq 1/2$ be arbitrary.
2. Compute the n points
$$T_1(z), T_2(z), \ldots, T_n(z).$$
Let z' be any one of these points with maximum imaginary part.
3. Let z'' be a translate of z' having $|\mathrm{Re}\,(z'')| \leq 1/2$.
4. If $\mathrm{Im}\,(z'') > \mathrm{Im}\,(z)$, then replace z by z'' and repeat from step 2.
5. If instead $\mathrm{Im}\,(z'') \leq \mathrm{Im}\,(z)$, then $z \in \mathcal{F}$, and we are done.

This process necessarily terminates after a finite number of steps, as is easily shown by using the fact that Γ acts properly discontinuously on $\mathcal{H}$ ([19, pp. 27, 31]). Note that the isometric circle $\mathfrak{I}(T)$ of $T = \left(\begin{smallmatrix} a & b \\ c & d \end{smallmatrix}\right)$ is given by $|cz+d| = 1$ and points inside $\mathfrak{I}(T)$ have $|cz+d| < 1$ while points outside $\mathfrak{I}(T)$ have $|cz+d| > 1$. This together with the fact that $\mathrm{Im}\,(Tz) = \mathrm{Im}\,(z)/|cz+d|^2$ shows that the algorithm will terminate with a point in $\mathcal{F}$.

4.5. **Further comments about accuracy.** Our computations are far too complicated for a rigorous error analysis. Instead we have made a number of tests that indicate what accuracy we can expect.

Our K-Bessel program is the foundation of all our computations, and the accuracy in our numbers depends very much on the accuracy in $K_{A+iR}(X)$. So naturally this is where we have made most of our tests. We have run a systematic test of comparisons between single and double precision on the Cray YMP-EL in various X- and R-ranges. Based on this comparison, we get the following results:

- $0 \leq R \leq 20$: 15 accurate places,
- $20 \leq R \leq 100$: 13–14 accurate places,
- $100 \leq R \leq 1000$: 11–13 accurate places,
- $1000 \leq R \leq 100000$: 9–11 accurate places.

Such a test assures us that we have internal self-consistency, but not that the computed value is in fact the correct one. This was instead checked by actually using the K-Bessel program to compute something we already knew the answer to. The zeros of the Riemann zeta-function made good guinea pigs for this. In fact, for $\Gamma_0(5)$ we have the formula (cf. [15, p. 538])

$$\varphi(s) := \det(\Phi(s)) = \pi \left[\frac{\Gamma(s-\frac{1}{2})}{\Gamma(s)} \frac{\zeta(2s-1)}{\zeta(2s)}\right]^2 \left(\frac{1-5^{2-2s}}{1-5^{2s}}\right). \tag{13}$$

Here $\Gamma(s)$ is the Gamma-function and $\zeta(s)$ is the Riemann zeta-function. (The notation $\varphi(s) := \det(\Phi(s))$ is customary for groups Γ with an arbitrary number of cusps, following [33]. Note that when the number of cusps is one, this agrees with (7).) We see that the zeros of $\zeta(2s-1)$ will also be zeros of $\varphi(s)$, and that they will be of order 2. It is believed that all zeros of the zeta-function are of the form $s = 1/2 + iT$. This means that the corresponding zeros of $\varphi(s)$ are $s = 3/4 + iT/2$. They were computed using the formula $\varphi(s) = \varphi^+(s)\varphi^-(s)$ mentioned in Section 3.

In searching for zeros of $\varphi(s)$, a good way of checking accuracy is the well-known relation $\varphi(s)\varphi(1-s) = 1$. Recall that zeros are found by integrating around a small rectangle enclosing the zero. If the zero is too close to one of the edges of the

rectangle, we have noticed that we lose accuracy due to "catastrophic cancellation" in the numerical quadrature of $\log \varphi(s)$. To avoid this, we always keep an eye on the size of $|\varphi(s)\varphi(1-s)-1|$. Typically this is between 10^{-12} and 10^{-14}, but it varies a great deal depending on the location of the zero. If the zero is close to $\mathrm{Re}\,(s) = 1/2$, it is automatically very close to the edge of the rectangle since the whole rectangle must be to the right of $\mathrm{Re}\,(s) = 1/2$. Therefore we expect zeros of $\varphi(s)$ lying close to $\mathrm{Re}\,(s) = 1/2$ to be less accurate.

In our algorithms, we have a choice of the parameters Y and M_0; see subsection 4.1. The result should be *independent* of these parameters, which is another (excellent) way of checking accuracy.

In Table 1, we show our computations of the zeros $s = 1/2 + iT$ of the Riemann zeta-function. We form these from the corresponding zeros, $\rho = 3/4 + iT/2$, of $\varphi(s)$ for $\Gamma_0(5)$. The values marked with $*$ are table values, correct in all decimals (except possibly the last one); cf., e.g., [26]. We show computations made with different values for Y and M_0, and we also display the maximum value δ of $|\varphi(s)\varphi(1-s)-1|$ over the four vertices of the rectangle of integration. We find that δ seems to be a good measure of our accuracy.

For the cusp form program, the *oldforms* provide good examples when checking accuracy. Oldforms can be found in Hejhal and Arno [14, p. 250] to 12–13 decimal places and even oldforms can be found in Steil [35] (also reprinted in [32, p. 207]) to 11 decimal places. We include here some of the values from these references along with our values; see Table 2. In the first column of these tables, we indicate the source of the eigenvalue. The values with no reference are ours, taken from Table 3 and [3]. The value ε indicates the expected accuracy of R (cf. [4, p. 51]), and e/o marks even or odd; cf. subsection 5.1. We find that our values show excellent agreement with [14] and [35].

The cusp forms have been computed using a variety of different values for Y_1, Y_2 and M_0. The results usually agree to the level indicated by ε.

Except for the testings of the K-Bessel function, which we ran on Uppsala University's Cray YMP-EL, all computations were made on computers with Athlon or Pentium processors running RedHat Linux. All code was written in Fortran. For the Athlon and Pentium machines, we used the GNU g77 compiler, and used the

TABLE 1. Comparison of computations of zeros of the zeta-function.

$\mathrm{Im}\,(s)$	M_0	Y	δ
14.1347251417346910	35	0.190	3.89E-14
14.1347251417346911	35	0.195	4.13E-14
14.1347251417346910	39	0.190	2.47E-14
*14.1347251417346938			
21.0220396387715666	39	0.190	5.25E-14
21.0220396387715560	39	0.195	2.95E-14
21.0220396387715631	46	0.190	2.90E-14
*21.0220396387715550			
25.0108575801456858	37	0.190	3.84E-14
25.0108575801456858	39	0.190	2.60E-14
25.0108575801457000	39	0.195	4.39E-14
*25.0108575801456888			
30.4248761258595160	39	0.190	4.72E-14
30.4248761258595088	41	0.190	6.52E-14
30.4248761258595088	41	0.195	4.47E-14
30.4248761258595088	46	0.190	5.30E-14
*30.4248761258595132			

TABLE 2. Comparison of eigenvalues of oldforms.

	R-value	ε	e/o
	9.5336952613535555	0.6217E-14	o
Hejhal and Arno [14]	9.5336952613536		
	12.173008324679640	0.5329E-14	o
Hejhal and Arno [14]	12.1730083246801		
	14.358509518259811	0.5329E-14	o
Hejhal and Arno [14]	14.358509518259		
	13.779751351890659	0.5329E-14	e
Hejhal and Arno [14]	13.7797513518907		
Steil [35]	13.77975135189		
	16.138073171521028	0.5329E-14	o
Hejhal and Arno [14]	16.138073171521		
	16.644259201899814	0.5329E-14	o
Hejhal and Arno [14]	16.6442592018999		
	17.738563381057375	0.5329E-14	e
Hejhal and Arno [14]	17.7385633810580		
Steil [35]	17.73856338106		
	19.423481470828257	0.5329E-14	e
Hejhal and Arno [14]	19.423481470828		
Steil [35]	19.42348147083		
	21.315795940203713	0.5329E-14	e
Hejhal and Arno [14]	21.3157959402041		
Steil [35]	21.31579594020		
	22.785908494189872	0.5329E-14	e
Hejhal and Arno [14]	22.785908494190		
Steil [35]	22.78590849419		
	35.841676432582829	0.3553E-14	e
Steil [35]	35.84167643258		
	41.555577673575214	0.3553E-14	e
Steil [35]	41.55557767358		
	47.926558330596521	0.7105E-14	e
Hejhal and Arno [14]	47.926558330595		
Steil [35]	47.92655833060		

data type "double precision" which is 64 bits wide (53 bits precision). On the Cray YMP-EL, we compiled with cf77, using the CRAY "single precision", which is 64 bits wide (48 bits precision).

5. Results

5.1. **Eigenvalues of cusp forms.** Recall that our aim is to compute and track poles of the Eisenstein series (and corresponding zeros of $\varphi(s)$) for groups Γ in the vicinity of $\Gamma_0(5)$. To know where to start looking for any newly created poles, we need to have good numerical values for the eigenvalues, $\lambda = 1/4 + R^2$, of cusp forms on $\Gamma_0(5)\backslash\mathcal{H}$.

We have computed the R-values of $\Gamma_0(5)$ cusp forms with $0 < R < 50$. In this range we have found 1029 R-values, of which 787 correspond to newforms, and the remaining 242 correspond to pairs of oldforms.

The method we used to localize the eigenvalues was essentially that of [16]. As in [40], Weyl's law can be used as an (experimental) reassuring test that we have a complete list of eigenvalues (cf. [41, p. 100] and [30, p. 101]; see also [4] for further explanation and plots).

The first 54 R-values are shown in Table 3. Here ε indicates the accuracy of R. The true R-value is expected to be within a distance $\pm\varepsilon$ of the value in the table (cf. [4, p. 51]). The last column gives the type of the eigenvalue; e/o indicates even

TABLE 3. The first 54 eigenvalues of $\Gamma_0(5)$ cusp forms.

R-value	ε	e/o $\pm$	R-value	ε	e/o $\pm$
3.0283762930658704	0.5773E-14	o −	10.500443150731548	0.5329E-14	o −
4.1032218099064535	0.5773E-14	o −	10.631153086564504	0.1155E-13	e −
4.1324042150631559	0.5773E-14	e +	10.983968954952880	0.5329E-14	o +
4.8972350157333597	0.5773E-14	o +	11.093128000485403	0.6217E-14	o −
5.4361804614158533	0.5773E-14	e −	11.153934934757895	0.6217E-14	o +
5.7058265271867965	0.5773E-14	o −	11.181381958034565	0.6217E-14	e +
6.0540283807717605	0.5773E-14	e +	11.283440679103108	0.6217E-14	e −
6.3512232167613973	0.5773E-14	o +	11.600538637136478	0.6217E-14	o −
6.4584764384814140	0.5773E-14	o −	11.692320734526873	0.5329E-14	e +
6.8235269954200453	0.5773E-14	e +	11.870849429961001	0.5329E-14	o +
7.3255243793270104	0.5773E-14	o +	12.018318517427783	0.6217E-14	e −
7.5853184014367230	0.5773E-14	o −	12.120773545866260	0.6217E-14	e +
7.9865490509824291	0.5773E-14	e −	*12.173008324679640	0.5329E-14	o
8.0184823783935268	0.6217E-14	o −	12.314171940441102	0.5329E-14	o −
8.2261459725999213	0.5329E-14	o +	12.636080054759094	0.5329E-14	e −
8.2946977835725253	0.5329E-14	e +	12.658506880380958	0.5329E-14	o +
8.4800158393978720	0.5329E-14	e +	12.715902144158203	0.5329E-14	o −
8.8178972986231408	0.6217E-14	o +	12.855458374568888	0.6217E-14	e +
8.8207408849461082	0.5329E-14	o −	13.000663851704766	0.1155E-13	e +
9.2772977852690701	0.6217E-14	e −	13.096388919221713	0.5329E-14	o −
9.3974175506637661	0.6217E-14	e −	13.219786079758204	0.6217E-14	o +
*9.5336952613535555	0.6217E-14	o	13.468981727907754	0.5329E-14	e +
9.6462667207114094	0.6217E-14	e +	13.575146972215373	0.1243E-13	o +
9.8334127366932886	0.5329E-14	o −	13.647394298454500	0.1155E-13	o +
10.045820825033910	0.5329E-14	o −	13.699306985217624	0.1155E-13	e −
10.246301380527013	0.5329E-14	e +	13.759948945063884	0.5329E-14	o −
10.307026865635046	0.6217E-14	o +	*13.779751351890659	0.5329E-14	e

and odd, $\pm$ indicates "type" $\phi(W_0 z) = \pm\phi(z)$ (cf. Section 2). Oldforms are marked with $*$, the others are newforms. The rest of the list can be found in [3] or [4].

5.2. **Destruction of cusp forms; first-order contact.** Our aim was to explore to what extent we can destroy the first 11 cusp forms listed in Table 3, along with two oldforms: $R_0 = 12.173008324680$ which is odd, and $R_0 = 13.779751351891$ which is even. We let $\Gamma_0(5)$ deform into a group Γ, and looked for zeros of $\varphi^+(s)$ or $\varphi^-(s)$ close to $1/2+iR$ for each R-value. For oldforms, the eigenspace corresponding to each eigenvalue is two-dimensional (cf. Section 2). This means that if an oldform is destroyed as we pass from $\Gamma_0(5)$ to Γ, we can expect to find *two* sets of zeros moving away from $\mathrm{Re}\,(s) = 1/2$, one for $\varphi^+(s)$ and one for $\varphi^-(s)$ (cf. also the remark regarding oldforms in subsection 5.4).

When one zero $\rho = 1/2 + \eta + i\gamma$ (or two for oldforms) was found for each R_0, we could, without too much effort, locate additional zeros by predicting their location with the Taylor expansions from Section 3. For convenience, we repeat them here (we again write $s_0 = 1/2 + iR_0$):

$$
\begin{aligned}
\eta =& A_1 a^2 + A_2(r-\tfrac{1}{5})^2 + A_3 a^2(r-\tfrac{1}{5}) + A_4(r-\tfrac{1}{5})^3 \\
&+ A_5 a^4 + A_6 a^2(r-\tfrac{1}{5})^2 + A_7(r-\tfrac{1}{5})^4 + A_8 a^4(r-\tfrac{1}{5}) \\
&+ A_9 a^2(r-\tfrac{1}{5})^3 + A_{10}(r-\tfrac{1}{5})^5 + A_{11} a^6 + \cdots, \\
\gamma =& R_0 + B_0(r-\tfrac{1}{5}) + B_1 a^2 + B_2(r-\tfrac{1}{5})^2 \\
&+ B_3 a^2(r-\tfrac{1}{5}) + B_4(r-\tfrac{1}{5})^3 + B_5 a^4 + \cdots.
\end{aligned} \tag{14}
$$

We proceeded using three different directions in $T(\Gamma_0(5))$:

(a')	:	a is varied and $r = \frac{1}{5}$ is kept constant
(r')	:	r is varied and $a = 0$ is kept constant
$(a'r')$	:	along $r = \frac{1}{5}(1-a)$

(a and r were defined in Section 2). For each zero found, we computed the pertinent coefficients in (14). All zeros and coefficients can be found in [6] and [4] along with explanations of how the coefficients are computed. Here we discuss just a few examples.

For directions (a') and $(a'r')$, we were able to find paths of zeros moving away from each one of the examined cusp forms, and also for (r') in the case of *even* R-values. In most cases, we found that the coefficients of (14) are nearly constant along the paths. An example where the coefficients computed for different zeros ρ agree very well is $R_0 = 3.0284$ and direction (a') (see also Figure 1):

a	r	$\mathrm{Re}\,(\rho)$	$\mathrm{Im}\,(\rho)$	A_1	B_1
0.000	0.2	0.50000000000000	3.02837629306587		
0.001	0.2	0.50000343891325	3.02838635724336	3.4389	10.0642
0.002	0.2	0.50001375518149	3.02841655026854	3.4388	10.0643
0.003	0.2	0.50003094738981	3.02846687361987	3.4386	10.0645
0.004	0.2	0.50005501317859	3.02853732976225	3.4383	10.0648

In some cases, however, we needed to compute high-order terms to see good agreement. Such an example is B_0 for $R_0 = 7.3255$ in direction $(a'r')$ (in this direction $A_1 + A_2/25$ is the coefficient of the lowest term in the expansion for η):

a	r	$\mathrm{Re}\,(\rho)$	$\mathrm{Im}\,(\rho)$	$A_1 + A_2/25$	B_0
0.000	0.2000	0.50000000000000	7.32552437932701		
0.005	0.1990	0.50148207183360	7.31726296496438	59.28	8.3
0.006	0.1988	0.50212664257926	7.31587615968384	59.07	8.0
0.007	0.1986	0.50288500720379	7.31456802423114	58.88	7.8
0.008	0.1984	0.50375654537815	7.31333462936287	58.70	7.6

We see here that $A_1+A_2/25$ agrees well for the different ρ-values, but B_0 is changing too much. The reason could be that higher coefficients in the Taylor expansion are needed here. To see if that will help, we compute the higher coefficients using pairs of zeros. Here the a-values indicate what pair was used to get each coefficient value. For η, the next coefficient up is $-A_3/5 - A_4/125$; for γ, it is $B_1 + B_2/25$. We see that the agreement in B_0 is now much better. Also $A_1 + A_2/25$ agrees better, and is probably closer to its true value.

a_1 a_2	$A_1 + A_2/25$	$-A_3/5 - A_4/125$	B_0	$B_1 + B_2/25$
7.32552437932701				
0.005 0.006	60.33	-209	9.37	44.25
0.006 0.007	60.25	-196	9.33	42.84
0.007 0.008	60.15	-182	9.28	41.47

Since $R_0 = 7.3255$ is *odd*, one actually has $A_2 = A_4 = 0$ in the above tables. The reason for this is that when we take $a = 0$ and vary r, i.e., move in direction (r'), the Eisenstein series will necessarily be *even* (cf. the next-to-last paragraph of Section 3). The deformation of *odd* cusp forms in direction (r') will thus never hit the "Eisenstein space", and one must *remain* in the setting of odd cusp forms. This is exactly what we find numerically: as we vary r, we are able to see cusp forms with R-values moving continuously away from the original one. Full data for these forms is given in [6] and [4]. (Some of these cases have also been studied by Farmer and Lemurell in [13].)

5.3. **Destruction of cusp forms; higher-order contact.** When we studied the overall accuracy of our coefficients, we found something very interesting. Namely, all of the *even* cusp forms showed very bad accuracy in their coefficient A_1. When we introduced higher-order terms in the expansion, we found that the reason appeared to be that we actually have $A_1 = 0$. When A_1 is *assumed* to be absent, the higher coefficients show excellent agreement.

This is strong evidence that we have a fourth-order contact for all *even* cusp forms in direction (a'). Indeed, in this direction $r \equiv 1/5$, and $(14)_\eta$ becomes

$$\eta = A_1 a^2 + A_5 a^4 + A_{11} a^6 + \cdots .$$

What we find is that this Taylor expansion appears to have $A_1 = 0$; i.e., it reads

$$\eta = A_5 a^4 + A_{11} a^6 + \cdots .$$

We include here $R_0 = 5.4362$ as an example. In these tables (for direction (a')), the coefficients A_5 and A_{11} that are marked with $'$ are computed *assuming* $A_1 = 0$. We see that they show much better agreement than the coefficients computed without this assumption.

a	r	$\mathrm{Re}\,(\rho)$	$\mathrm{Im}\,(\rho)$	A_1	A_5'
0.000000	0.2	0.50000000000000	5.43618046141585		
0.002875	0.2	0.50000011881445	5.43586528969062	0.0144	1739
0.003000	0.2	0.50000014082502	5.43583731552122	0.0156	1739
0.004000	0.2	0.50000044387798	5.43557089539080	0.0277	1734
0.004500	0.2	0.50000070984652	5.43540934042368	0.0351	1731
0.005000	0.2	0.50000107994933	5.43522895720637	0.0432	1728

a_1	a_2	A_1	A_5	A_5'	A_{11}'
5.43618046141585					
0.0030	0.0040	0.000096	1728	1744.6	-668875
0.0040	0.0045	0.000216	1720	1744.5	-665709
0.0045	0.0050	0.000336	1714	1744.5	-663194

In Figure 1 (right) we show a plot of the real part of these zeros along with the curves of $1/2 + A_1 a^2$ and $1/2 + A_5 a^4$ (with $A_1 = 0.0144$, $A_5 = 1744.6$). We see that the zeros appear to lie on the fourth-order curve. The figure also shows the

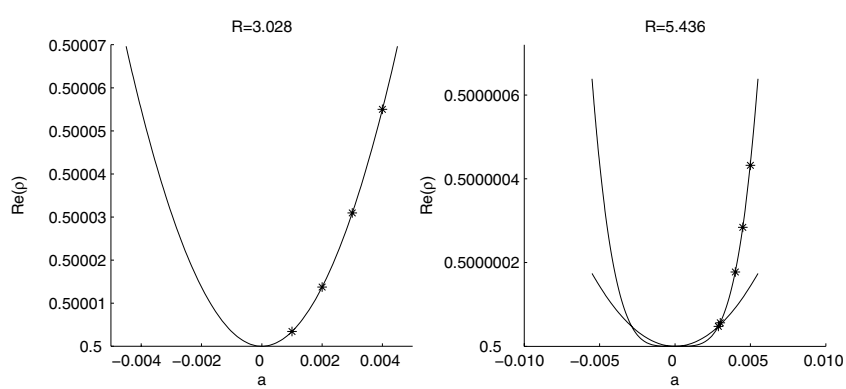

FIGURE 1. Zeros ρ found near the cusp forms having $R_0 = 3.028$ and $R_0 = 5.436$ for direction (a'). $\mathrm{Re}\,(\rho)$ is plotted as a function of the parameter a. The curve in the first plot is $1/2 + 3.4389a^2$. The curves in the second plot are $1/2 + 0.0144a^2$ and $1/2 + 1744.6a^4$. We see that the zeros appear to lie on the fourth-order curve.

analogous situation for $R_0 = 3.028$, here with the curve $1/2 + A_1 a^2$, $A_1 = 3.4389$ shown. In this case a second-order curve fits the data very well (cf. [2] for more plots like these).

From our experiments we conclude that $A_1 = 0$. This can in fact be proved rigorously, at least under the assumption $A_2 \neq 0$ (as pointed out to me by Andreas Strömbergsson). The proof uses the Fricke involution symmetry and the formula by Phillips and Sarnak [29] for the second-order term in $(14)_\eta$. To see this, let $\phi(z)$ be a Maass cusp form for $\Gamma_0 = \Gamma_0(5)$ with eigenvalue $\lambda = 1/4 + R^2$. We assume that $\phi(z)$ is real valued and that λ is a simple eigenvalue. Let $Q(z) \not\equiv 0$ be any holomorphic cusp form of weight 4 on Γ_0, and let Γ_t, $t \to 0$, be the corresponding real-analytic deformation of Γ_0, as in [27, 29]. We write $\rho(t) = 1/2 + \eta(t) + i\gamma(t)$ for the corresponding zero of $\varphi(s)$, or if $\eta = 0$, we write the cusp form eigenvalue as $\frac{1}{4} + \gamma(t)^2$, (i.e., the corresponding element of the singular set $\sigma(\Gamma_0)$ is $\gamma + i\eta$). Since (a, r) form real-analytic coordinates on the Teichmüller space $T(\Gamma_0)$ near $(a, r) = (0, \frac{1}{5})$ (cf. [5]), we have (up to conjugation) $\Gamma_t = \Gamma_{a(t),r(t)}$ for some real-analytic curve $(a(t), r(t))$ with $(a'(0), r'(0)) \neq (0, 0)$. Hence by (14),

$$\eta''(0) = 2A_1 a'(0)^2 + 2A_2 r'(0)^2. \tag{15}$$

We will prove that $Q(z) \not\equiv 0$ can be chosen so that $\eta''(0) = 0$. Since $A_1, A_2 \geq 0$, it follows that at least one of A_1 and A_2 must vanish.

By Phillips and Sarnak [29, (5.29)] (cf. [27, Thm. 2.1]) we have

$$\eta''(0) = C \sum_{p \in \{i\infty, 0\}} \left| \int_{\Gamma_0 \backslash \mathcal{H}} \operatorname{Re}\big(Q(z) \cdot \Lambda^2 \phi(z)\big) \cdot E_p\left(z; \tfrac{1}{2} + iR\right) d\mu(z) \right|^2, \tag{16}$$

where $\Lambda = y^2 \frac{\partial}{\partial \bar{z}}$ and C is a fixed positive constant (recall that $i\infty, 0$ are the two cusps of Γ_0). As in [27, (3.1)] we define

$$F_p(s) = \int_{\Gamma_0 \backslash \mathcal{H}} \big(Q(z) \cdot \Lambda^2 \phi(z)\big) \cdot E_p(z; s)\, d\mu(z). \tag{17}$$

Recalling the properties of the Fricke involution $W_0(z) = -\frac{1}{5z}$ (cf. Section 2 and (10)) we see that we have $E_0(z; s) = E_{i\infty}(W_0 z; s)$ and $\phi(W_0 z) = \varepsilon_1 \phi(z)$, $Q(W_0 z) = \varepsilon_2 (\sqrt{5} z)^4 Q(z)$ for some $\varepsilon_1, \varepsilon_2 = \pm 1$, and hence $F_{i\infty}(s) = (\varepsilon_1 \varepsilon_2) \cdot F_0(s)$. It now follows from (16), (17) that

$$\eta''(0) = \frac{C}{2} \cdot \left| F_{i\infty}\left(\tfrac{1}{2} + iR\right) + \overline{F_{i\infty}\left(\tfrac{1}{2} - iR\right)} \right|^2. \tag{18}$$

From the definition of $F_p(s)$ and the fact that

$$\Phi(s) = \frac{1}{2} \begin{pmatrix} \varphi^+(s) + \varphi^-(s) & \varphi^+(s) - \varphi^-(s) \\ \varphi^+(s) - \varphi^-(s) & \varphi^+(s) + \varphi^-(s) \end{pmatrix},$$

one also computes

$$F_{i\infty}(s) = \begin{Bmatrix} \varphi^+(s) & \text{if } \varepsilon_1 \varepsilon_2 = 1 \\ \varphi^-(s) & \text{if } \varepsilon_1 \varepsilon_2 = -1 \end{Bmatrix} \cdot F_{i\infty}(1 - s).$$

In particular we have $|F_{i\infty}(1/2 + iR)| = |F_{i\infty}(1/2 - iR)|$. Hence there exists some non-zero complex number α for which

$$\alpha F_{i\infty}(1/2 + iR) + \overline{\alpha F_{i\infty}(1/2 - iR)} = 0.$$

And so by (18), if we replace Γ_t to be the deformation corresponding to αQ instead of Q, we have $\eta''(0) = 0$. This completes the proof that $A_1 = 0$ or $A_2 = 0$ must hold.

Note that *if* there exists a smooth nonsingular curve $(a(t),r(t))$ with $\eta(a(t),r(t)) \equiv 0$, as predicted by Farmer and Lemurell [13], then $A_1 = 0$ implies, using (15), that $r'(0) = 0$. That means that the curve $(a(t), r(t))$ is parallel to the a-axis, which is precisely what Farmer and Lemurell find experimentally.

5.4. **Comparison of Taylor coefficients.** In the preceding examples, we have looked at Taylor coefficients obtained while deforming Γ along *one* of the directions (a'), (r') or $(a'r')$. It is also interesting to make a comparison of coefficients between the three directions. For example, B_0 can be computed from direction (r') as well as from direction $(a'r')$, and one might want to compare the results. This comparison is shown in Tables 4 and 5. When looking at these tables one should keep in mind the following remarks:

- The coefficient values shown here are all taken from our computations using *pairs* of zeros because these are likely to be more accurate (i.e., the numbers are taken from Tables 3, 4, 7, 8, 11 in [6]).
- The columns are marked with (a'), (r') or $(a'r')$ to show which one of these three directions in $T(\Gamma_0(5))$ was under consideration.
- In the first column we show the type of the eigenvalue; e/o denotes even and odd, $\pm$ "type" $\phi(W_0 z) = \pm\phi(z)$ (cf. Section 2).
- The lowest coefficient for η in direction $(a'r')$ is $A_1 + A_2/25$; cf. (14). For *odd* cusp forms we necessarily have $A_2 = 0$, so then we get $A_1 + A_2/25 = A_1$, and we may compare this to A_1 as computed in direction (a'). This is done in columns 2 and 3 of Table 4.
- Using $A_1 = 0$ for even cusp forms, we may compute A_2 from the coefficient $A_1 + A_2/25$ found along direction $(a'r')$. In column 4 of Table 4 we show A_2 computed in this way, and we mark it A_2'. One may compare this to A_2 computed in direction (r') in column 5.
- In Table 5, for γ, we seek to compare the B_1-values from direction (a') and the B_2-values from direction (r') with the result from direction $(a'r')$, which is $B_1 + B_2/25$. We therefore form the expression $B_1 + B_2/25$ utilizing the direction (a') and direction (r') results from columns 4 and 5 of Table 5. This sum is denoted by $(a')+(r')$.

We find that *most* of the coefficients agree very well. Only some of the values for $B_1 + B_2/25$ for γ do not agree quite as much (see columns 6 and 7 in Table 5). The reason for this is almost certainly that we have not tracked the zero ρ close enough into $\mathrm{Re}\,(s) = 1/2$. Recall that the Taylor expansion (14) is valid close to $(a, r) = (0, 1/5)$ and $s = 1/2 + iR_0$, but we never know *how* close a priori. The good agreement of the analogous coefficients for η in the "bad" cases is, however, reassuring.

Recall from subsection 4.5 that we quickly lose accuracy when we approach $\mathrm{Re}\,(s) = 1/2$. To avoid some of this loss we may decrease the step size in the numerical quadrature at the cost of speed. It becomes a struggle between *needing* to find zeros closer to $\mathrm{Re}\,(s) = 1/2$ on one hand, and loosing accuracy and speed on the other. Several weeks of computer time were spent on finding zeros of $\varphi(s)$.

TABLE 4. Comparison of Taylor coefficients from (14) for η over the three directions (a'), (r'), and $(a'r')$.

1	2	3	4	5
R_0	A_1	A_1	A_2'	A_2
	(a')	$(a'r')$	$(a'r')$	(r')
3.0284 o−	3.44	3.44	-	0.0
4.1032 o−	49.2	48.9	-	0.0
4.1324 e+	-	-	364	364
4.8972 o+	0.0035	0.0027	-	0.0
5.4362 e−	-	-	244.8	244.9
5.7058 o−	13.5	13.7	-	0.0
6.0540 e+	-	-	2118	2117
6.3512 o+	7.7	8.0	-	0.0
6.4585 o−	11.2	11.2	-	0.0
6.8235 e+	-	-	1075	1086
7.3255 o+	60.5	60.3	-	0.0
12.1730 o+	23.1	23.0	-	0.0
12.1730 o−	81.62	81.63	-	0.0
13.7798 e+	-	-	1837	1843
13.7798 e−	-	-	6788	6788

TABLE 5. Comparison of Taylor coefficients from (14) for γ over the three directions (a'), (r'), and $(a'r')$.

1	2	3	4	5	6	7
R_0	B_0	B_0	B_1	B_2	$B_1 + \frac{B_2}{25}$	$B_1 + \frac{B_2}{25}$
	(r')	$(a'r')$	(a')	(r')	$(a')+(r')$	$(a'r')$
3.0284 o−	17.65	17.65	10.06	94	13.8	14.0
4.1032 o−	0.57	0.52	18.28	469	37	35
4.1324 e+	-17.06	-17.06	0.056	-134	-5.3	-5.4
4.8972 o+	11.4	11.3	-1.160	-4.7	-1.3	-2.7
5.4362 e−	-4.77	-4.77	-38.17	19.3	-37	-36
5.7058 o−	-16.3	-16.4	33.63	-117	28.9	24.3
6.0540 e+	0.63	0.65	10.37	326	23.4	24.3
6.3512 o+	16.2	16.2	-41.07	269	-30	-35
6.4585 o−	-0.79	-0.81	-7.29	200	0.71	0.46
6.8235 e+	2.6	2.5	21.7	-470	2.9	-1.0
7.3255 o+	9.5	9.4	38.21	49	40	44
12.1730 o+	27.27	27.27	1.69	-517	-19	-21
12.1730 o−	-28.1	-28.1	88.69	-6052	-153	-142
13.7798 e+	4.56	4.60	446	10396	860	914
13.7798 e−	-2.60	-2.60	427	4275	598	614

For the oldforms, each $\phi^{\pm}(z)$ is of multiplicity one in its respective symmetry class. Therefore it is not surprising that we find such good agreement of Taylor coefficients for 12.1730 and 13.7798. This is just a consequence of the real-analyticity of elements of the singular set for multiplicity one cusp forms (cf. Section 3).

The constancy of the coefficients along each path and the good agreement of the same coefficient computed along different paths strongly suggest that (except for the case of odd cusp forms in direction (r') explained above), each of our "starting" cusp forms *is* destroyed when $\Gamma_0(5)$ is deformed along directions (a'), (r') and $(a'r')$.

We have collected our approximated values of the coefficients $A_1, \ldots, A_5$ and $B_0, \ldots, B_2$ on a web-page [7].

5.5. **Nondestruction along a curve?** So far we have discussed destruction of cusp forms along straight lines in our parameterization of the Teichmüller space

$T(\Gamma_0(5))$. Recall that (14) will provide information regarding the possibility of destruction in a complete neighborhood of $(a, r) = (0, 1/5)$.[2]

Our starting point here is Lemma 3.1. Recall that a sufficient condition for a cusp form to be destroyed in all directions is that $d_1 = 4A_2A_5 - A_3^2 > 0$, and that from Farmer and Lemurell [13] we have reason to believe that $d_1 = 0$.

One naturally wonders if the investigation of possible nondestruction along a curve can be carried further using higher-order Taylor coefficients. By further analysis along the lines of Lemma 3.1 one can prove that there exists an infinite series of "discriminants" $d_1, d_2, d_3, \ldots$ (these are polynomials in the coefficients A_j, with $d_1 = 4A_2A_5 - A_3^2$) such that *either* $d_1 = d_2 = d_3 = \cdots = 0$, and then there is a curve along which $\eta(a, r) = 0$, *or else* there is some n such that $d_1 = d_2 = \cdots = d_{n-1} = 0$ and $d_n > 0$, in which case $\eta(a, r) > 0$ in some (punctured) neighborhood of $(a, r) = (0, 1/5)$.

In ongoing joint work with A. Strömbergsson where we aim at developing more efficient algorithms for the numerical study of the spectrum as Γ varies in Teichmüller space, we have computed the first few of these discriminants. This was done by combining the present methods for computation of Eisenstein series with the methods for high precision computations of Maass forms developed in [9]. (Test runs with the programs used for the earlier results of this paper were promising but could not offer the desired precision because we need to compute zeros very close to $\mathrm{Re}\,(s) = 1/2$.) All our results so far support the existence of the curves predicted by Farmer and Lemurell: For $R = 5.4362$ our numerics have shown $d_1 < 10^{-14}$ and d_2 and d_3 have been seen to vanish to at least 10 and 3 significant digits, respectively. We also note that the problematic Taylor coefficients in Table 5 (e.g., $B_1 + \frac{B_2}{25}$ for $R = 6.9235$) all seem to resolve nicely as higher precision allows us to carry out computations closer to the central point $(a, r) = (0, \frac{1}{5})$.

Recently P. Sarnak, when presented with our experimental findings, pointed out to us an approach which should make it possible to prove the existence of the curves predicted by Farmer and Lemurell, using the pseudo-Laplacian operator Δ_a introduced by Colin de Verdiere [10, 11] and working in the framework of [27]. The zeroth Fourier coefficient of the eigenfunctions of Δ_a, when normalized correctly, is a one-dimensional real parameter which vanishes only for *true* cusp forms. The point is that it should be possible to prove that this parameter (unlike the parameter $\eta = \eta(a, r)$ in Lemma 3.1) takes both positive and negative values; the desired conclusion will then follow by using the intermediate value theorem. We hope to give the details of this argument in a later publication (in progress).

Acknowledgments

The author is most grateful to Dennis Hejhal, David Farmer, Stefan Lemurell, Fredrik Strömberg and Andreas Strömbergsson for helpful discussions on this work.

References

[1] A. O. L. Atkin and J. Lehner, *Hecke operators on* $\Gamma_0(m)$, Math. Ann. **185** (1970), 134–160. MR0268123(42:3022)

[2] H. Avelin, *Research announcement on the deformation of cusp forms*, U.U.D.M. Report 2002:26, Uppsala, 21 pp., 2002.

[3] ———, *Computer programs and data*, 2003, `http://www.math.uu.se/staff/pages/?uname=helen`.

[2] The actual size of this neighborhood has to be determined experimentally.

[4] ———, *On the deformation of cusp forms*, U.U.D.M. Report 2003:8, Uppsala, 85 pp., 2003.

[5] ———, *Some computations used to prove that $\Gamma_{a,r}$ is a Fuchsian group*, 2004, Maple-file `http://www.math.uu.se/staff/pages/?uname=helen`.

[6] ———, *Zeros and coefficients*, 2004, `http://www.math.uu.se/staff/ pages/?uname=helen`.

[7] ———, *Values of taylor coefficients*, 2005, `http://www.math.uu.se/staff/pages/?uname=helen`.

[8] L. Bers, *Uniformization, moduli, and Kleinian groups*, Bull. London Math. Soc. **4** (1972), 257–300. MR0348097 (50:595)

[9] A. Booker, A. Strömbergsson, and A. Venkatesh, *Effective computations with Maass forms*, `http://www.math.uu.se/~astrombe/ papers.html`, preprint, 2005.

[10] Y. Colin de Verdiere, *Pseudo-Laplacians I*, Ann. Inst. Fourier **32** (1983), no. 3, 275–286. MR0688031 (84k:58221)

[11] ———, *Pseudo-Laplacians II*, Ann. Inst. Fourier **33** (1983), no. 2, 87–113. MR0699488 (84k:58222)

[12] A. Erdélyi, W. Magnus, F. Oberhettinger, and F. G. Tricomi, *Higher Transcendental Functions*, vol. 2, McGraw–Hill, 1953. MR0698780 (84h:33001b)

[13] D. W. Farmer and S. Lemurell, *Deformations of Maass forms*, Math. Comp. **74** (2005). MR164106

[14] D. A. Hejhal and S. Arno, *On Fourier coefficients of Maass waveforms for $PSL(2,\mathbb{Z})$*, Math. Comp. **61** (1993), 245–267 and S11–S16. MR1199991 (94a:11062)

[15] D. A. Hejhal, *The Selberg Trace Formula for $PSL(2,\mathbb{R})$*, vol. 2, Lecture Notes in Math. **1001**, Springer-Verlag, Berlin, 1983. MR711197 (86e:11040)

[16] ———, *Eigenvalues of the Laplacian for Hecke Triangle Groups*, Mem. Amer. Math. Soc. (1992), no. 469, 165pp. MR1106989 (93f:11043)

[17] ———, *On eigenfunctions of the Laplacian for Hecke triangle groups*, Emerging Applications of Number Theory (D. Hejhal, J. Friedman, M. Gutzwiller, and A. Odlyzko, eds.), Springer-Verlag, 1999, pp. 291–315. MR1691537 (2000f:11063)

[18] H. Iwaniec, *Introduction to the Spectral Theory of Automorphic Forms*, Biblioteca de la Revista Matemática Iberoamericana, 1995. MR1325466 (96f:11078)

[19] S. Katok, *Fuchsian Groups*, The University of Chicago Press, Chicago, 1992. MR1177168 (93d:20088)

[20] B. Maskit, *On Poincaré's theorem for fundamental polygons*, Adv. in Math. **7** (1971), 219–230. MR0297997 (45:7049)

[21] M. H. Millington, *On cycloidal subgroups of the modular group*, Proc. London Math. Soc. **3** (1969), 164–176. MR0248232 (40:1484)

[22] T. Miyake, *On automorphic forms on GL_2 and Hecke operators*, Ann. Math. **94** (1971), 174–189. MR0299559 (45:8607)

[23] ———, *Modular Forms*, Springer-Verlag, 1989. MR2194815 (2006g:11084)

[24] J. Marklof and A. Strömbergsson, *Equidistribution of Kronecker sequences along closed horocycles*, Geom. funct. anal. **13** (2003), 1239–1280. MR2033838 (2005d:37011)

[25] S. Nag, *The complex analytic theory of Teichmüller spaces*, John Wiley & Sons, Inc., 1988. MR0927291 (89f:32040)

[26] A. M. Odlyzko and A. Schönhage, *Fast algorithms for multiple evaluations of the Riemann zeta function*, Trans. Amer. Math. Soc. **309** (1988), no. 2, 797–809. MR0961614 (89j:11083)

[27] R. S. Phillips and P. Sarnak, *On cusp forms for cofinite subgroups of $PSL(2,\mathbb{R})$*, Invent. Math. **80** (1985), 339–364. MR0788414 (86m:11037)

[28] ———, *The Weyl theorem and the deformation of discrete groups*, Comm. Pure Applied Math. **38** (1985), no. 6, 853–866. MR0812352 (87f:11035)

[29] ———, *Perturbation theory for the Laplacian on automorphic functions*, J. Amer. Math. Soc. **5** (1992), 1–32. MR1127079 (92g:11056)

[30] M. S. Risager, *Asymptotic densities of Maass newforms*, J. Number Theory **109** (2004), no. 1, 96–119. MR2098479 (2006b:11049)

[31] A. Ralston and P. Rabinowitz, *A First Course in Numerical Analysis*, 2nd ed., McGraw–Hill, Tokyo, 1978. MR1828483 (2001k:65001)

[32] P. Sarnak, *Arithmetic quantum chaos*, Israel Math. Conf. Proc. **8** (1995), 183–236. MR1321639 (96d:11059)

[33] A. Selberg, *Harmonic analysis and discontinuous groups in weakly symmetric Riemannian spaces with applications to Dirichlet series*, J. Indian Math. Soc. B. **20** (1956), 47–87. MR0088511 (19,531g)

[34] ———, *Göttingen Lectures on Harmonic Analysis*, in Collected Papers, vol. 1, Springer-Verlag, 1989, pp. 626–674.

[35] G. Steil, *Eigenvalues of the Laplacian and of the Hecke Operators for* $PSL(2,\mathbb{Z})$, DESY report 94-028, 1994.

[36] F. Strömberg, *Computations of Maass waveforms in non-congruence subgroups of the modular group*, in Computational aspects of Maass waveforms, Ph.D. Thesis, Uppsala University, Uppsala, Sweden, 2005, pp. 107–123.

[37] A. Strömbergsson, *An application of an explicit trace formula to a well-known spectral correspondence on quaternion groups*, 2000, Chapter 3 of Ph.D. Thesis, `http://www.math.uu.se/~astrombe/papers.html`.

[38] ———, *A pullback algorithm for general (cofinite) Fuchsian groups.*, 2000, `http://www.math.uu.se/~astrombe/papers.html`, technical note.

[39] ———, *Some remarks on a spectral correspondence for Maass waveforms*, Internat. Math. Res. Notices (2001), no. 10, 505–517. MR1832538 (2002h:11045)

[40] H. Then, *Arithmetic quantum chaos of Maass waveforms*, Ulm Report ULM-TP/03-4, Ulm, 30 pp., 2003.

[41] A. B. Venkov, *Spectral Theory of Automorphic Functions*, Proc. Steklov Inst. Math. **153** (1982), no. 4, 1–163. MR0692019 (85j:11060b)

[42] G. N. Watson, *A Treatise on the Theory of Bessel Functions*, 2nd ed., Cambridge University Press, Cambridge, 1944. MR0010746 (6,64a)

Department of Mathematics, Uppsala University, Box 480, S-751 06 Uppsala, Sweden
E-mail address: `helen.avelin@math.uu.se`